

Epitaxial Growth of Omega-Titanium on the (111) Surface of Alpha-Iron

Yang-Tse Cheng* and Wen-Jin Meng

Physics and Physical Chemistry Department, General Motors Research and Development Center, Warren, Michigan 48090
(Received 29 November 1995)

ω -Ti films of trigonal structure are grown epitaxially on the (111) surface of α -Fe at 300 K by electron beam evaporation in UHV. The ω -Ti films are oriented with the (0001) plane parallel to the α -Fe(111) plane and the ω -Ti $[2\bar{1}\bar{1}0]$ direction in the α -Fe $[1\bar{1}0]$ direction in the plane of the substrate. The second-nearest-neighbor atomic interaction is believed responsible for the formation of ω -Ti at the interface. The relatively thick ω -Ti film (40 nm) is a result of the small energy difference between ω -Ti and the competing hcp-Ti. [S0031-9007(96)00259-1]

PACS numbers: 68.35.Bs, 81.15.Kk

Epitaxial growth of metallic thin films is an actively pursued area of research for fundamental studies of thin film growth processes and for applications in novel electronic and magnetic devices [1]. One of the fundamental issues is the formation of metastable phases by epitaxial growth. Examples include the formation of body-centered-cubic (bcc) Cu on bcc Fe [2], face-centered-cubic (fcc) Co or Fe on fcc Cu [3], and fcc Cr on Au [4]. In these cases, the overlayer adopts a crystal structure that is well lattice matched to the substrate and is normally different from that the overlayer material would have in the bulk. This phenomenon, known as pseudomorphism, has recently attracted both experimental and theoretical investigations [1–5]. Usually, the pseudomorphic overlayer can grow to a few monolayers before transforming to equilibrium phases. An exception is the epitaxial growth of bcc Co on GaAs [6]. The thickness of bcc Co can reach 35 nm before the film transforms to its bulk hexagonal-close-packed (hcp) structure. The lattice mismatch between the bcc Co and GaAs substrate is very small (0.4%). Subsequent electronic structure calculations show that the bcc Co is a metastable state which lies about 5 mRy above the ground state [7]. In this Letter, we report, for the first time, the epitaxial growth of the trigonal structure ω -Ti on the (111) surface of bcc Fe (α phase) at 300 K by electron beam evaporation in UHV. The lattice mismatch between ω -Ti and α -Fe is about 12%. Despite the large lattice mismatch, the thickness of the ω -Ti film is about 40 nm. This observation may stimulate a broad interest in solid state physics, including epitaxial thin films, phase transformations, and total energy calculations of bulk and interface structures.

This study was motivated by our previous observations that, at 300 K, (a) (111) oriented α -Fe films can grow epitaxially on hydrogen terminated Si(111) substrates [8] and (b) double hcp-Nd can grow epitaxially on the (111) surface of α -Fe [9]. Titanium was chosen to further explore epitaxial growth, since there is a large lattice mismatch between hcp Ti and α -Fe (about 31%). Furthermore, bulk Ti can exist in several forms. At normal pressure, it transforms from hcp (α phase) to bcc (β phase) at high tem-

perature. At room temperature, Ti transforms from α to the ω phase under high pressure [10]. Recently, a partial α - to ω -phase transformation induced in Ti during ion irradiation in the electronic slowing-down regime has been reported [11]. The formation of epitaxial ω -Ti films has, to the best of our knowledge, not been reported.

A [111] oriented α -Fe film was first deposited on hydrogen terminated Si(111) substrates at 300 ± 3 K under similar conditions as described previously [8]. Then, a Ti film was deposited onto the α -Fe(111)/Si(111) structure from an electron beam evaporation source in the same UHV chamber and at the same substrate temperature. The base pressure was better than 3×10^{-9} Torr and the pressure remained in the low 10^{-8} Torr range during deposition. The Ti deposition rate was 0.05 nm/s from a 99.99% pure Ti source (AESAR). Before exposing the samples to air, a 15 nm thick Si layer was deposited on top of some of the samples to prevent oxidation of the Ti and Fe layers in air. Sputter depth profiles obtained using a 4 keV Ar^+ ion beam and x-ray photoelectron spectroscopy showed that the oxygen and carbon contamination in the bulk of the films was less than the detection limit of 1 at.%. The interfaces between Ti and Fe, between Fe and Si, and between the Si cover layer and Ti were well defined, without evidence of interdiffusion.

Figure 1(a) is a θ - 2θ x-ray diffraction (XRD) pattern of a 50 nm thick Ti film on a 35 nm thick α -Fe(111) on a Si(111) substrate. All films were deposited at 300 K. In addition to the substrate Si peaks and the α -Fe(222) peak, the two observed diffraction peaks correspond to a plane spacing of 0.2818 and 0.1410 nm, respectively. These peaks cannot be identified with either hcp ($a = 0.29505$ nm and $c = 0.46826$ nm) [12] or bcc Ti ($a = 0.33065$ nm) [13]. Nor can they be identified with known Ti hydrides [14], including δ hydride (CaF_2 structure), ϵ hydride TiH_2 [face-centered-tetragonal (fct) structure, with $c/a < 1$], and γ hydride (fct with $c/a > 1$). These diffraction peaks do not match various Ti oxides either, consistent with the observation that the oxygen concentration in the films is less than 1 at.%.

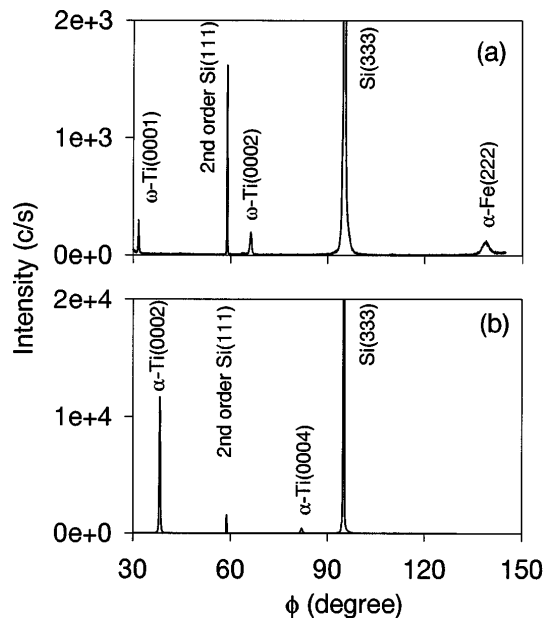


FIG. 1. θ - 2θ x-ray diffraction patterns of a 50 nm thick Ti layer on a 35 nm thick α -Fe(111) layer on a Si(111) substrate (a) and a 50 nm thick Ti layer on an oxidized Si(111) surface (b).

They can be identified, however, with the ω -Ti (0001) and (0002) diffraction, knowing the unit cell constants for ω -Ti ($0.4621 < a < 0.4643$ nm and $0.2810 < c < 0.2819$ nm) [10].

It is well established that the ω phase can exist in two slightly different modifications, hexagonal (ideal ω) and trigonal (rumpled ω), with space group D_{6h}^1 ($P6/mmm$) and D_{3d}^3 ($P\bar{3}m1$), respectively [10,15]. The positions of the atoms in the ω structure can be written $(0,0,0)$ and $\pm(1/3, 2/3, 1/3 + \delta)$ with $0 < \delta \leq 1/6$. For $\delta \neq 1/6$ the crystal is trigonal, and for $\delta = 1/6$ the crystal has the hexagonal symmetry. The geometrical structure factor is given by

$$F_{hkl} = 1 + 2 \cos 2\pi[(h - k + l)/3 + l\delta]. \quad (1)$$

The crystal structure of the films is further examined by XRD ϕ scans. With the x-ray incident angle set at 16.168° and detector angle at 54.869° from the sample plane, three diffraction peaks are observed as the sample rotated 360° about the sample norm [Fig. 2(a)]. The corresponding 2θ is 71.037° and d spacing is 0.1327 nm. The d spacing can be identified with that of the $\{10\bar{1}2\}$ planes of ω -Ti. Furthermore, the angle between the norm of these planes and the sample norm is 19.350° , which is the expected angle between $\{10\bar{1}2\}$ and $\{0001\}$ of ω -Ti. Since the structure factor is zero for the respective hexagonal but nonzero for the trigonal ω -Ti $\{10\bar{1}2\}$ diffractions, the structure of the Ti film deposited at 300 K on the (111) surface of α -Fe is that of the trigonal ω -Ti.

According to Eq. (1), there can be six $\{10\bar{1}2\}$ diffractions in the above ϕ scan for the trigonal ω -Ti. The struc-

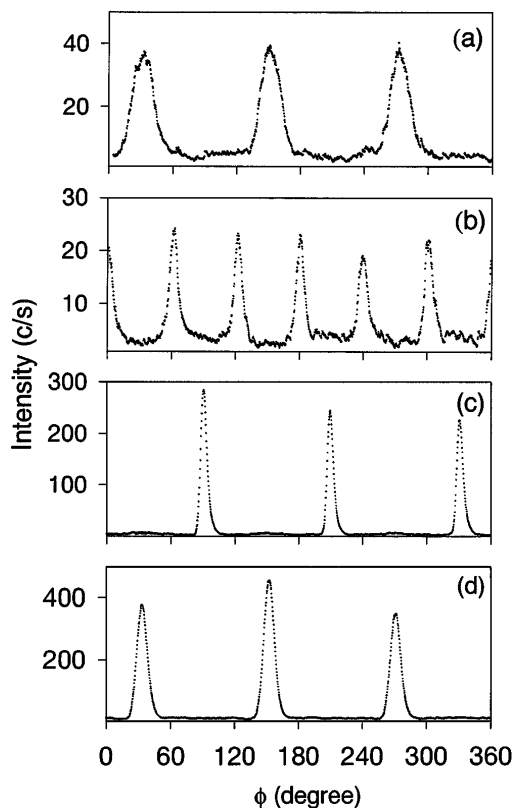


FIG. 2. XRD ϕ scans of the ω -Ti $\{10\bar{1}2\}$ diffraction (a), the ω -Ti $\{11\bar{2}2\}$ diffraction (b), the α -Fe $\{202\}$ diffraction (c), and the α -Fe $\{211\}$ diffraction (d) of a 50 nm thick Ti film on a 35 nm thick Fe film on Si(111).

ture factor for three of the six is $1 + 2 \cos 4\pi\delta$ and for the other three is $1 + 2 \cos 2\pi(1/3 + 2\delta)$. Since three $\{10\bar{1}2\}$ diffraction peaks are observed in the above ϕ scan [Fig. 2(a)], we can estimate δ to be less than $1/14$ from the structure factor and measured scattering intensity.

Consistent with Eq. (1), six ω -Ti $\{11\bar{2}2\}$ diffractions are also observed using XRD ϕ scan with the x-ray incident angle set at 8.596° and detector angle at 71.213° from the sample plane [Fig. 2(b)]. This set of peaks and their azimuthal angular position with respect to the set of $\{10\bar{1}2\}$ diffraction peaks [Fig. 2(a)] provide further evidence that the film is ω -Ti.

The ω -Ti film is grown epitaxially on the (111) surface of α -Fe, evident from XRD θ - 2θ scan for Ti [Fig. 1(a)], and ϕ scans for ω -Ti and α -Fe (Fig. 2). Since three peaks of ω -Ti $\{10\bar{1}2\}$ diffraction, 120° from each other, are located halfway between the α -Fe $\{202\}$ peak positions and are aligned with α -Fe $\{211\}$ peak positions [Figs. 2(a)–2(d)], the following in-plane orientation relationship is obtained [Fig. 3(a)]:

$$(0001)_{\omega\text{-Ti}} \parallel (111)_{\alpha\text{-Fe}} \text{ with } [2\bar{1}\bar{1}0]_{\omega\text{-Ti}} \parallel [1\bar{1}0]_{\alpha\text{-Fe}}. \quad (2)$$

Also depicted are two alternative orientation relationships that are not observed [Figs. 3(b) and 3(c)].

The *in situ* reflection high energy electron diffraction (RHEED) patterns [Figs. 4(a)–4(d)] provide additional evidence for ω -Ti and the above orientation relationship [Eq. (2)]. The transmission diffraction patterns from ω -Ti [Figs. 4(c) and 4(d)] are also consistent with that simulated using the Cerius² software [16]. Furthermore, RHEED results show that (1) epitaxy is initiated at the interface between Ti and Fe and (2) the ω -Ti film can grow to a thickness of about 30 to 40 nm before the appearance of hcp-Ti. The latter observation is consistent with the coherence length of 40 nm determined by XRD for Ti films 50 nm thick.

The observed ω -Ti films are metastable with respect to the commonly observed α -Ti (hcp) in the following sense. (1) XRD and *in situ* RHEED experiments show that, at the same substrate temperature of 300 K, the hcp-Ti gradually appears with increasing thickness of the ω -Ti. This gradual transition occurs when the thickness of the ω -Ti film is about 30 to 40 nm. (2) The hcp-Ti films are observed when Ti is deposited on α -Fe(111) surfaces at higher temperatures (e.g., 450 K). (3) Annealing of an ω -Ti film formed at 300 K at high temperatures, such as at 373 K for 1 h in UHV, causes a significant decrease in x-ray scattering intensity of the ω -Ti phase and an increase in intensity of the hcp Ti. At room temperature, however, the ω -Ti thin film of about 50 nm thickness covered with 15 nm thick Si is stable for at least 4 yr, as shown by the identical XRD results obtained during the time period. (4) At the substrate temperature of 300 K, hcp-Ti films always form when Ti is deposited on many substrates, including oxidized silicon substrates [Fig. 1(b)]. The latter also shows that

epitaxy is responsible for the formation of the ω -Ti films on Fe(111) surfaces.

To elucidate the growth mechanisms, it may be instructive to consider the structures of Ti. From the symmetry point of view, there is little advantage for Ti to take on the trigonal structure (ω) when it is deposited on the (111) surface of α -Fe, since either bcc or hcp phases can grow epitaxially on the (111) surface of bcc metals [17]. From the lattice mismatch point of view, the mismatch between the $\{2\bar{1}\bar{1}0\}$ planes of hcp Ti and the $\{110\}$ planes of α -Fe is very large, $(d_{\alpha\text{-Fe}}^{\{110\}} - d_{\text{hcp-Ti}}^{\{2\bar{1}\bar{1}0\}})/d_{\text{hcp-Ti}}^{\{2\bar{1}\bar{1}0\}} = -31.3\%$ or $(2d_{\alpha\text{-Fe}}^{\{110\}} - d_{\text{hcp-Ti}}^{\{2\bar{1}\bar{1}0\}})/d_{\text{hcp-Ti}}^{\{2\bar{1}\bar{1}0\}} = 37.3\%$. The lattice mismatch between the $\{110\}$ planes of bcc-Ti and bcc-Fe is about -13.3% . The lattice mismatch between $\{2\bar{1}\bar{1}0\}$ planes of ω -Ti and $\{110\}$ planes of α -Fe, $(2d_{\alpha\text{-Fe}}^{\{110\}} - d_{\omega\text{-Ti}}^{\{2\bar{1}\bar{1}0\}})/d_{\omega\text{-Ti}}^{\{2\bar{1}\bar{1}0\}}$, is about -12.4% . This large lattice mismatch is only slightly smaller than that between bcc-Ti and bcc-Fe (-13.3%). Furthermore, the lattice mismatch would be the same for either the hexagonal or trigonal ω -Ti on bcc Fe(111). Accordingly, simple symmetry or lattice mismatch considerations based on two-dimensional surface nets alone cannot explain the epitaxial growth of the trigonal ω -Ti on the Fe(111) surface.

The three epitaxial relationships depicted in Fig. 3 have the same two-dimensional surface net with identical lattice mismatch. The main difference between them is the plane spacing in the (0001) direction, which affects the second-nearest-neighbor distance between Ti and Fe atoms near the interface. The fact that only one of these orientations is observed shows that the second-nearest-neighbor atomic interaction is essential in determining the formation of the epitaxial ω -Ti thin films.

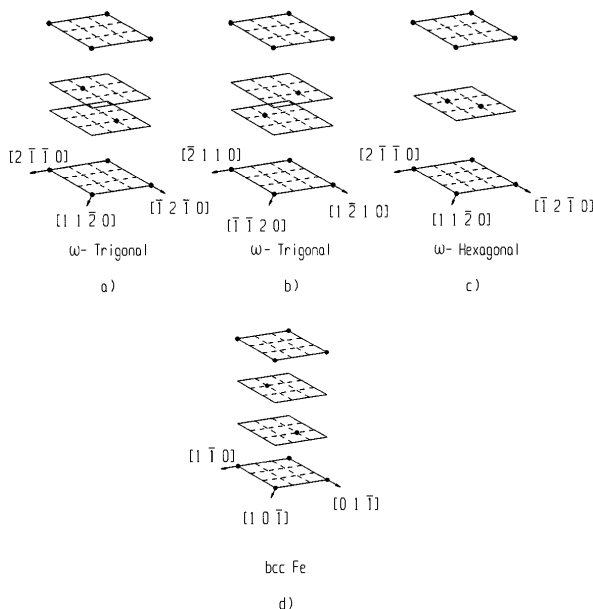


FIG. 3. An illustration of the structure and orientation relationships between trigonal ω -Ti (a) and (b), hexagonal ω -Ti (c), and α -Fe (d).

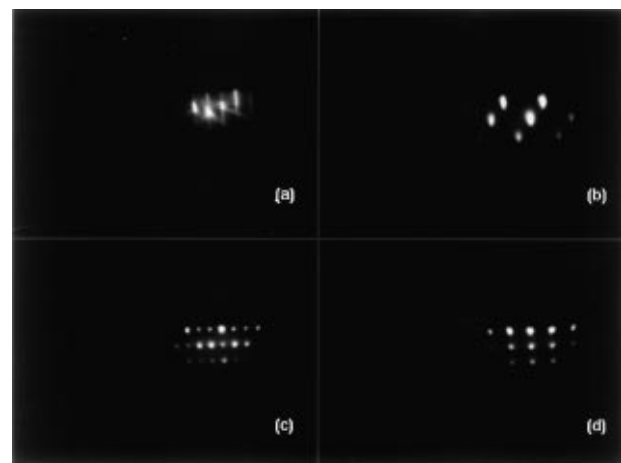


FIG. 4. RHEED patterns taken along $[\bar{1}\bar{1}0]$ Si (a), along the same direction when Fe is 15 nm thick (b) and when Ti is 27 nm thick (c), and along $[\bar{2}\bar{1}\bar{1}]$ Si when Ti is 27 nm thick (d). The pattern (b) is consistent with that of the $[\bar{1}\bar{1}0]$ α -Fe transmission diffraction pattern. The patterns (c) and (d) are consistent with that of the $[2\bar{1}\bar{1}0]$ and $[10\bar{1}0]$ ω -Ti transmission diffraction patterns, respectively.

While the thickness of the previously observed metastable metal films made by epitaxy is usually a few atomic layers, the thickness of the ω -Ti is about 40 nm. Furthermore, the lattice mismatch is large compared to the cases of pseudomorphism. The relatively thick metastable ω -Ti films are perhaps a result of the very small energy difference between ω -Ti and the competing hcp-Ti phase. According to recent first-principles, total energy calculations [18], with ω -Ti has a slightly lower energy than the hcp structure at zero temperature. The present experiment shows that the ω -Ti film is metastable at room temperature. However, the small energy difference could explain the relatively thick ω -Ti film on Fe(111).

Future experiments include the investigation of the possible influence of strain in this unusual case of epitaxial growth. It would also be instructive to calculate the electronic structure and interfacial energy for various Ti/Fe interfaces. Recently, Ezaki *et al.* have shown, using a discrete-variational cluster method, that adding transition metals of higher valence electrons, such as Fe, into Ti is effective in strengthening the atomic bonds in the bulk ω -Ti phase [19]. The present observation indicates that the same situation may also be true for the Ti atoms at the Ti/Fe interface. Furthermore, considering the small energy difference between bulk ω - and hcp-Ti, the lowest interfacial energy configuration may be that observed in this experiment.

We would like to thank S. J. Simko and M. C. Militello for XPS measurements and R. A. Waldo for electron microprobe analysis. Discussions with R. Blint, Y.-L. Chen, G. L. Eesley, G. B. Fisher, C. D. Fuerst, W. A. Goddard, J. P. Heremans, J. F. Herbst, G. P. Meisner, F. E. Pinkerton, A. Poli, J. R. Smith, D. D. Snyder, and K. C. Taylor have also been helpful.

*Electronic address: cheng@gmr.com

[1] E. G. Bauer, B. W. Dodson, D. J. Ehrlich, L. C. Feldman, C. P. Flynn, M. W. Geis, J. P. Harbison, R. J. Matyi, P. S. Peercy, P. M. Petroff, J. M. Phillips, G. B. Stringfellow, and A. Zangwill, *J. Mater. Res.* **5**, 852 (1990).

[2] I. A. Morrison, K. H. Kang, and E. J. Mele, *Phys. Rev. B* **39**, 1575 (1989).

[3] D. A. Steigerwald and W. F. Egelhoff, Jr., *Surf. Sci.* **192**, L887 (1987); C.-A. Chang, *Appl. Phys. Lett.* **58**, 1745 (1991).

[4] S. M. Durbin, L. E. Berman, B. W. Batterman, M. B. Brodsky, and H. C. Hamaker, *Phys. Rev. B* **37**, 6672 (1988).

[5] R. Bruinsma and A. Zangwill, *J. Phys. (Paris)* **47**, 2055 (1986); P. Beauchamp and J. P. Villain, *J. Phys. (Paris)* **44**, 1117 (1983).

[6] G. A. Prinz, *Phys. Rev. Lett.* **54**, 1051 (1985).

[7] P. M. Marcus and V. L. Moruzzi, *Solid State Commun.* **55**, 971 (1985).

[8] Y.-T. Cheng, Y.-L. Chen, M. M. Karmarkar, and W.-J. Meng, *Appl. Phys. Lett.* **59**, 953 (1991); *Phys. Rev. B* **48**, 14 729 (1993).

[9] Y.-T. Cheng and Y.-L. Chen, *Appl. Phys. Lett.* **60**, 1951 (1992).

[10] J. C. Jamieson, *Science* **140**, 72 (1963); S. K. Sikka, Y. K. Vohra, and R. Chidambaram, *Prog. Mater. Sci.* **27**, 245 (1982); H. Xia, G. Parthasarathy, H. Luo, Y. K. Vohra, and A. L. Ruoff, *Phys. Rev. B* **42**, 6736 (1990).

[11] H. Dammak, A. Barbu, A. Dunlap, D. Lesueur, and N. Lorenzelli, *Philos. Mag. Lett.* **67**, 253 (1993).

[12] X-ray Powder Diffraction File No. 44-1294 (JCPDS-ICDD, Swarthmore, 1994).

[13] X-ray Powder Diffraction File No. 44-1288 (JCPDS-ICDD, Swarthmore, 1994).

[14] For example, S. R. Peddada, I. M. Robertson, and H. K. Birnbaum, *J. Mater. Res.* **8**, 291 (1993); Y. Kasukabe, Y. Yamada, and L. A. Bursill, *Philos. Mag.* **67**, 73 (1993).

[15] S. L. Sass, *J. Less-Common Met.* **28**, 157 (1972); D. T. Keating and S. J. LaPlaca, *J. Phys. Chem. Solids* **35**, 879 (1974).

[16] Cerius², Molecular Simulations, Burlington, Massachusetts.

[17] Y.-T. Cheng and Y.-L. Chen, *J. Mater. Res.* **7**, 1567 (1993); J. C. A. Huang, R. R. Du, and C. P. Flynn, *Phys. Rev. Lett.* **66**, 341 (1991).

[18] R. Ahuja, J. M. Wills, B. Johansson, and O. Eriksson, *Phys. Rev. B* **48**, 16 269 (1993).

[19] H. Ezaki, M. Morinaga, M. Kato, and N. Yukawa, *Acta Metall.* **39**, 1755 (1991).